

Polycrystalline CdS/CdTe solar cells

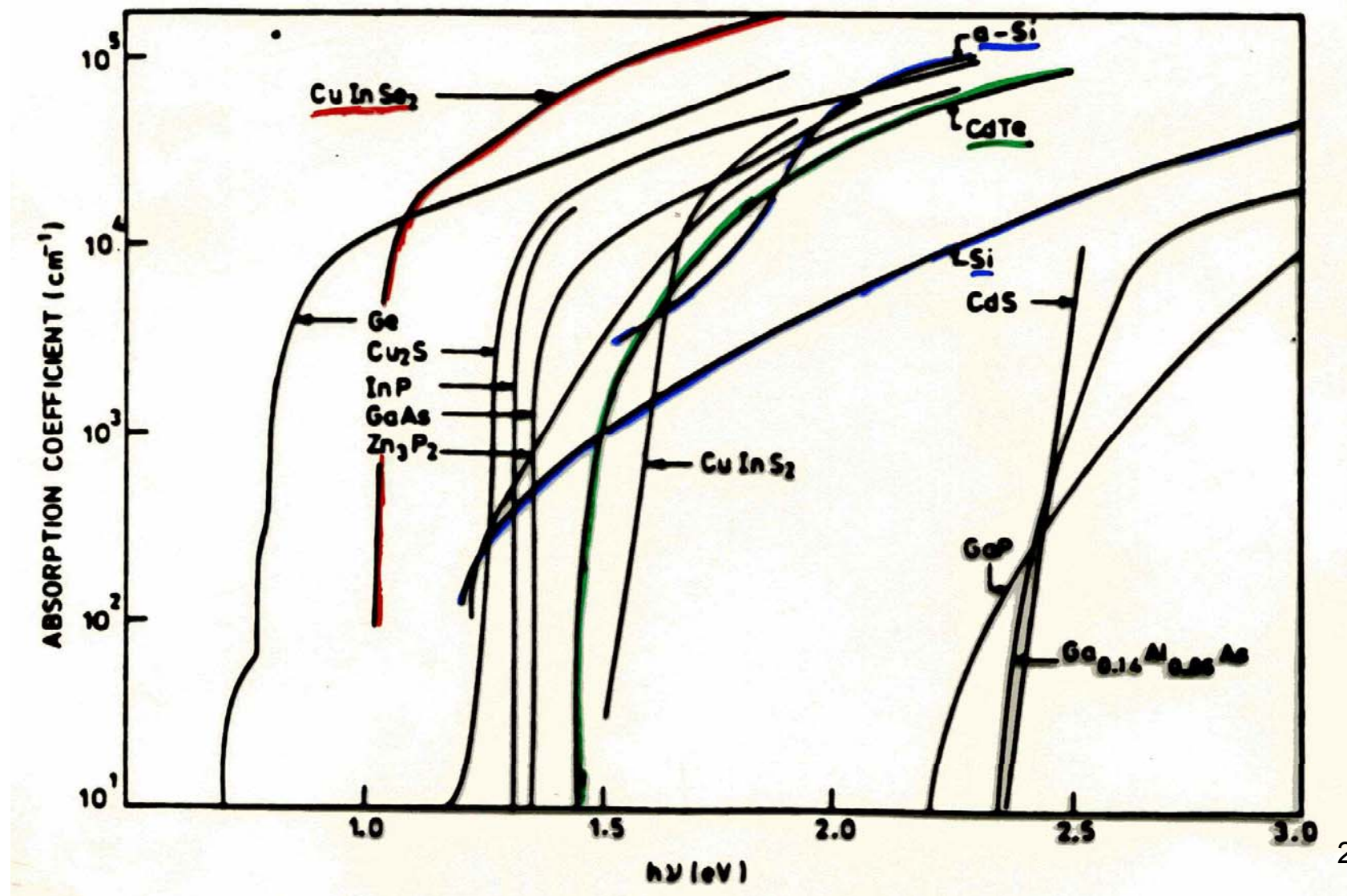
Al Compaan

Distinguished University Professor of Physics, Emeritus

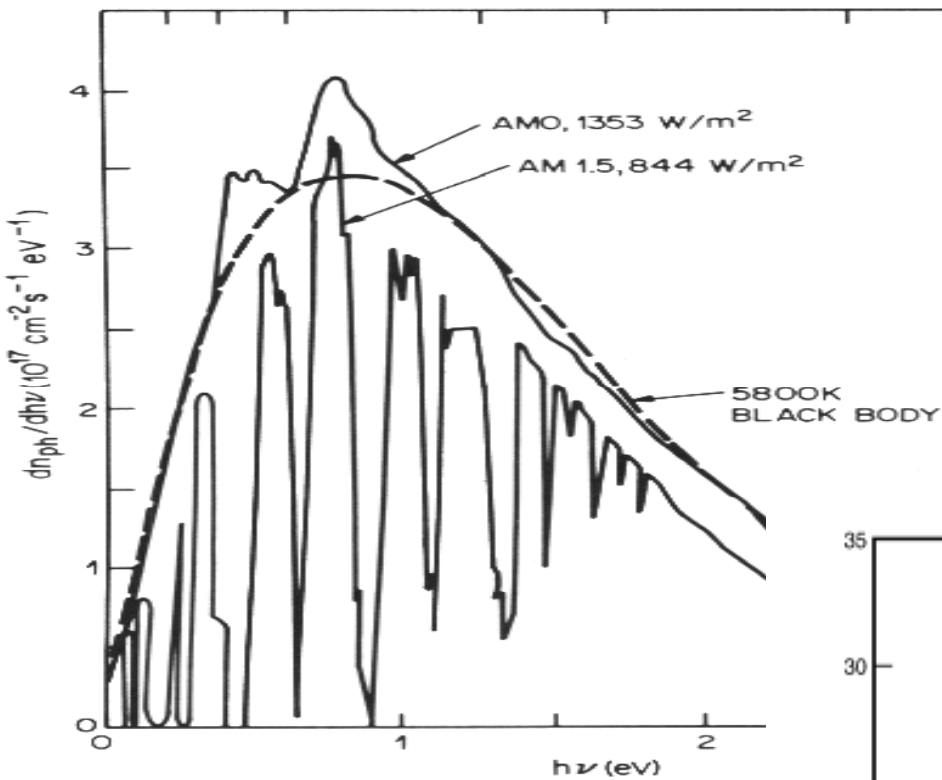
(Lecture for Heben/Ellingson solar cells class)

March 3, 2011

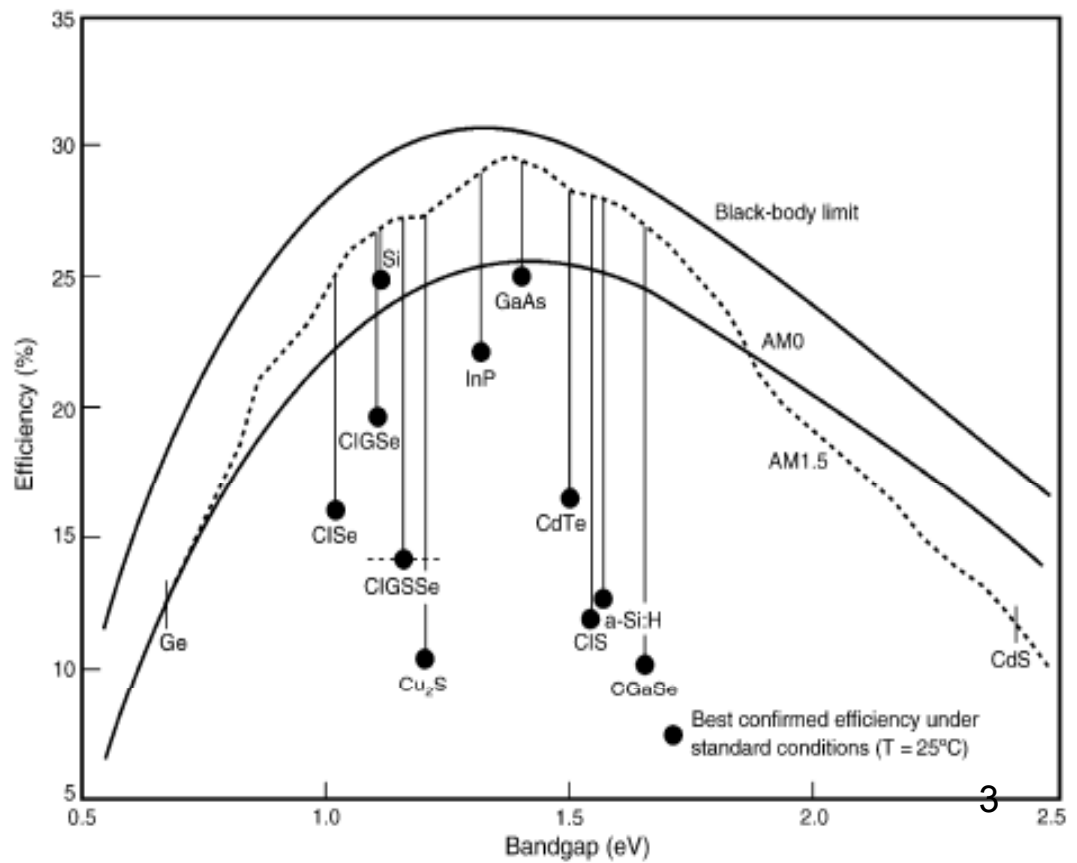
Absorption spectra of various semiconductors



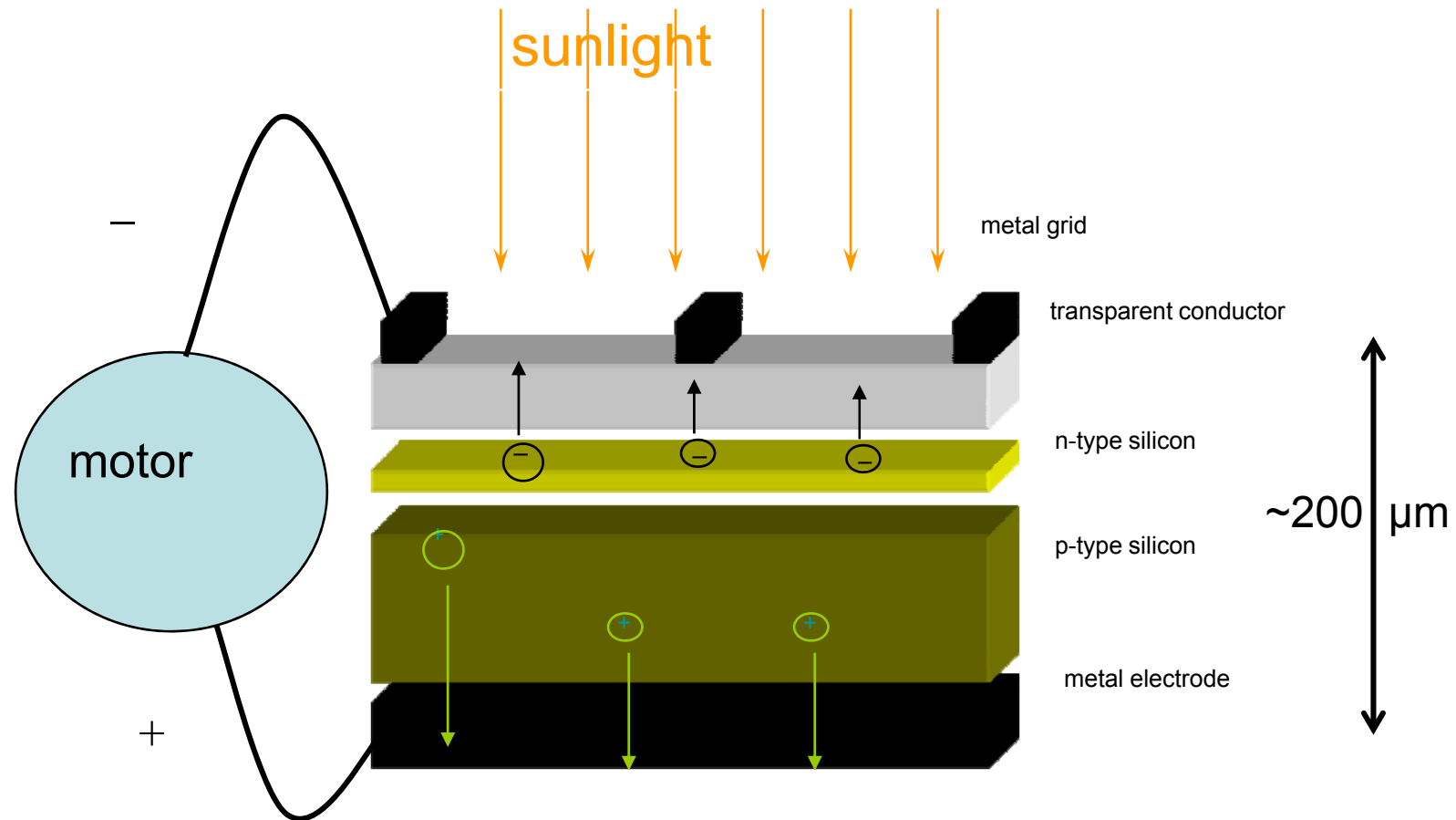
actual and attainable single junction cell efficiencies (inorganic materials)



Attainable cell efficiencies for AM0 (solid line) and AM1.5 spectra (dashed line) and best efficiencies achieved for several materials as single junctions. (Kazmerski 2006)

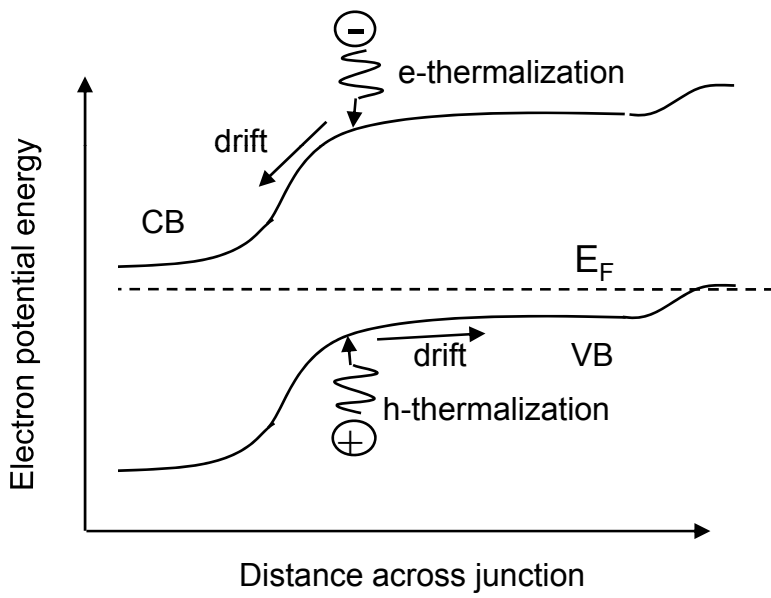
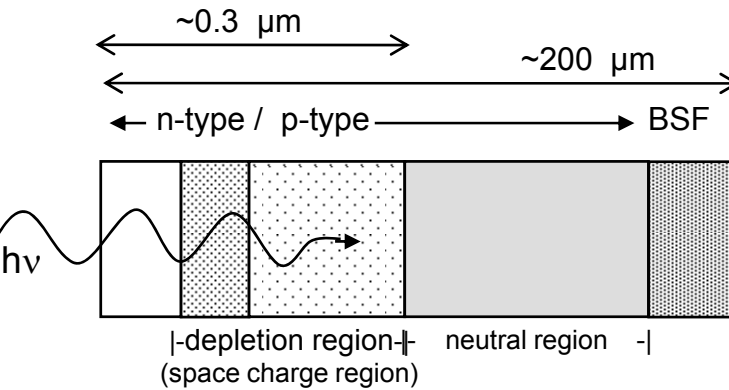
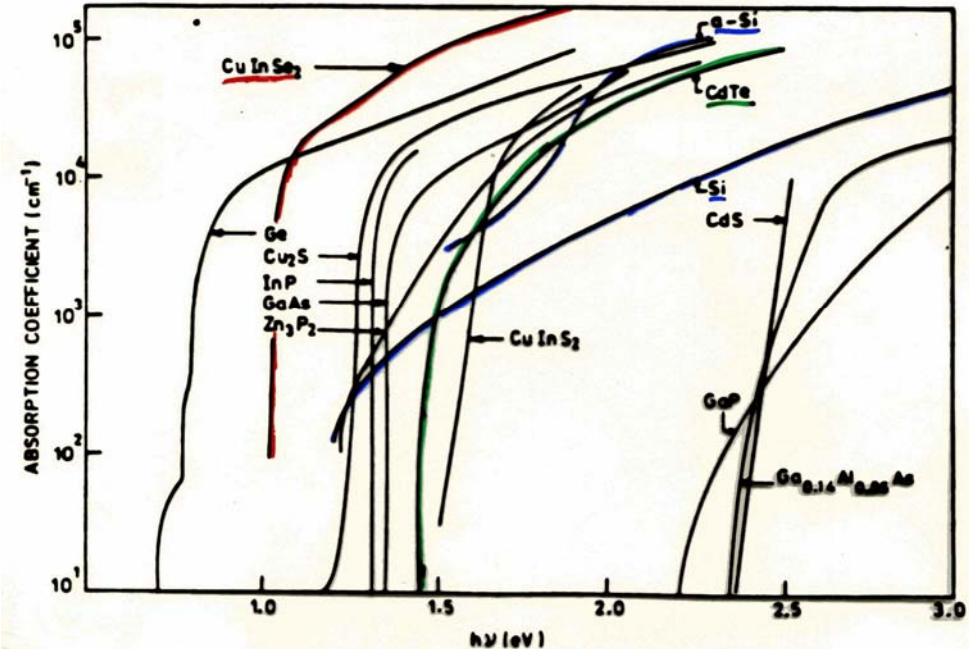


the traditional silicon solar cell



band diagram for a homojunction (n on p)

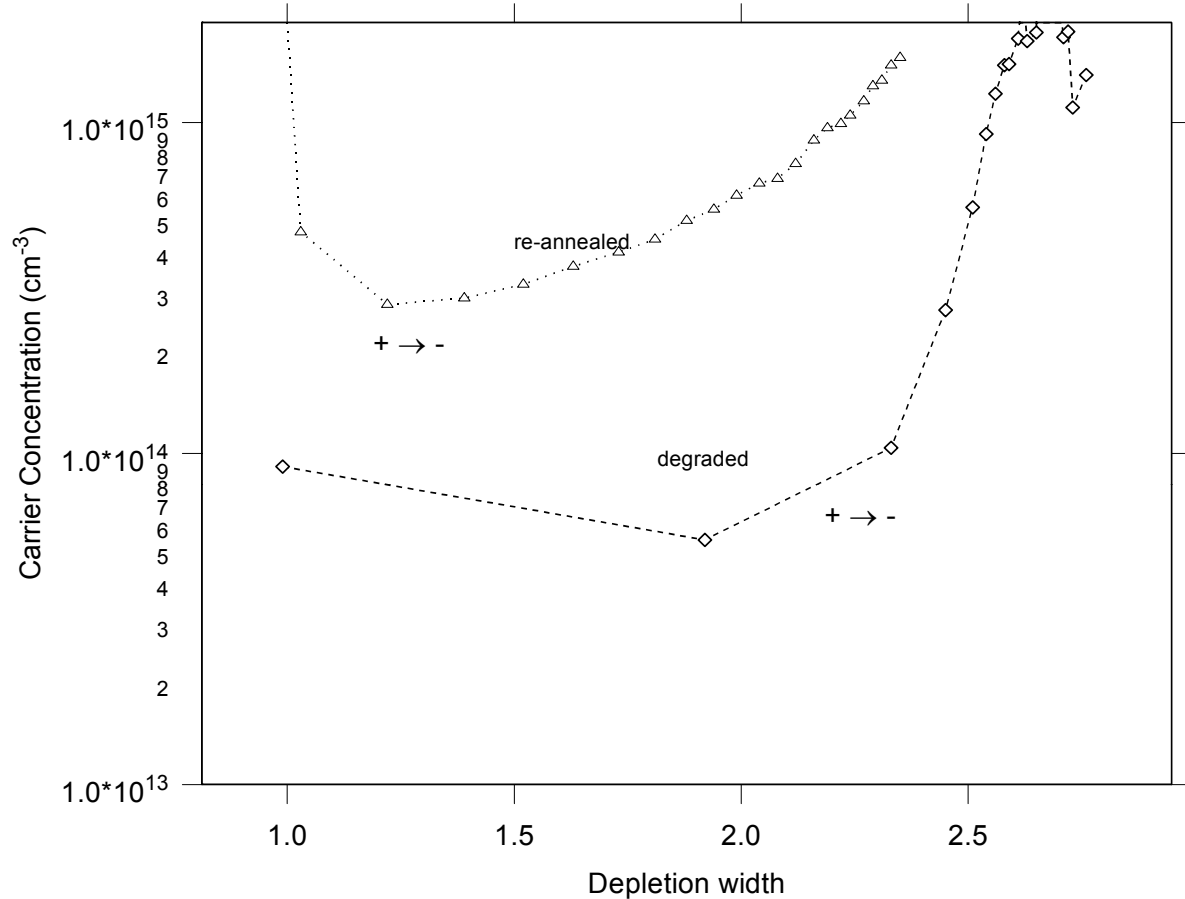
- Si (indirect band gap) will have typically a thick neutral region-- carrier collection by diffusion
- most thin-film (direct band gap materials) will have mostly field-assisted collection



Solar cell structure and energy band diagram showing valence (VB) and conduction bands (CB), Fermi level (E_F), photoabsorption, electron-hole pair generation, thermalization, and drift.
(from Compaan, APS News April, 2005)

C-V measurements of depletion width in CdS/CdTe cells

CdTe is difficult to
dope p-type
extrinsically



Depletion width in a single-sided step junction:

$$W = \{(2K\epsilon_0 V_{bi}) / qN_a\}^{1/2}$$

(for Si with $N_a = 1 \times 10^{16} \text{ cm}^{-3}$, $W \approx 0.35 \mu\text{m}$)

Construct a band diagram of the CdS/CdTe solar cell....

What information do we need?

J. Appl. Phys., Vol. 87, No. 3, 1 February 2000

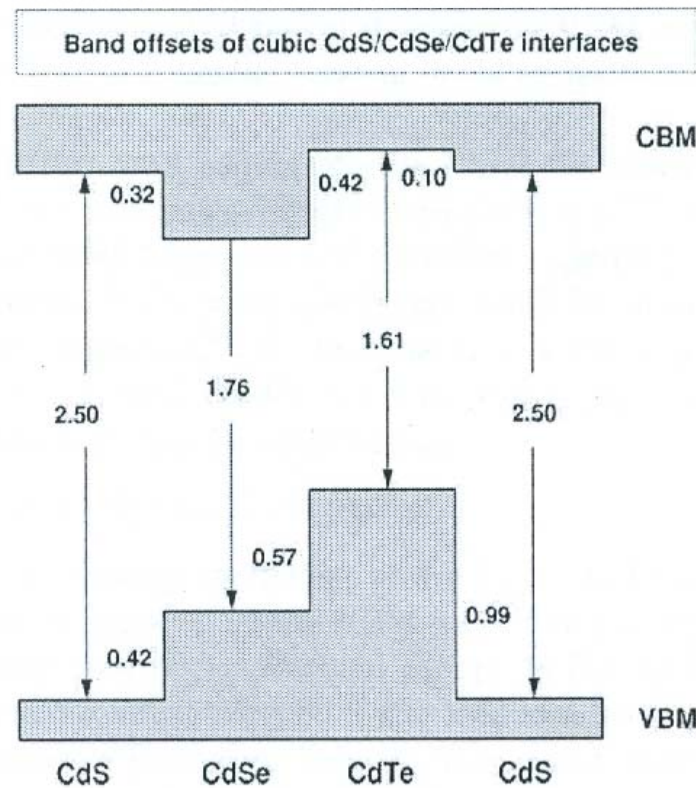


FIG. 2. Calculated natural valence band and conduction band offsets for interfaces between Cd-based compounds.

S-H Wei, S.B. Zhang, A. Zunger (T = 0 K band gaps)

Electron affinity of CdTe
 $E_a = 5.6 \text{ eV}$

Work functions of common metals

Metal	Work Functions		
		(eV)	(V)
Ag (silver)	4.26		
Al (aluminum)	4.28 see notes		
Au (gold)	5.1		
Cs (cesium)	2.14		
Cu (copper)	4.65		
Li (lithium)	2.9		
Pb (lead)	4.25		
Sn (tin)	4.42		
Chromium	4.6		
Molybdenum	4.37		
Stainless Steel	4.4		
Gold	4.8		
Tungsten	4.5		
Copper	4.5		7
Nickel	4.6		

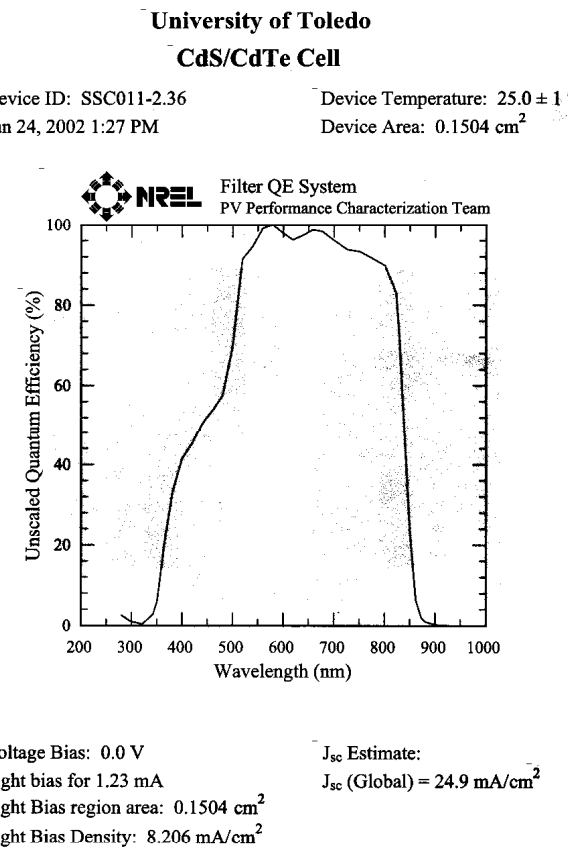
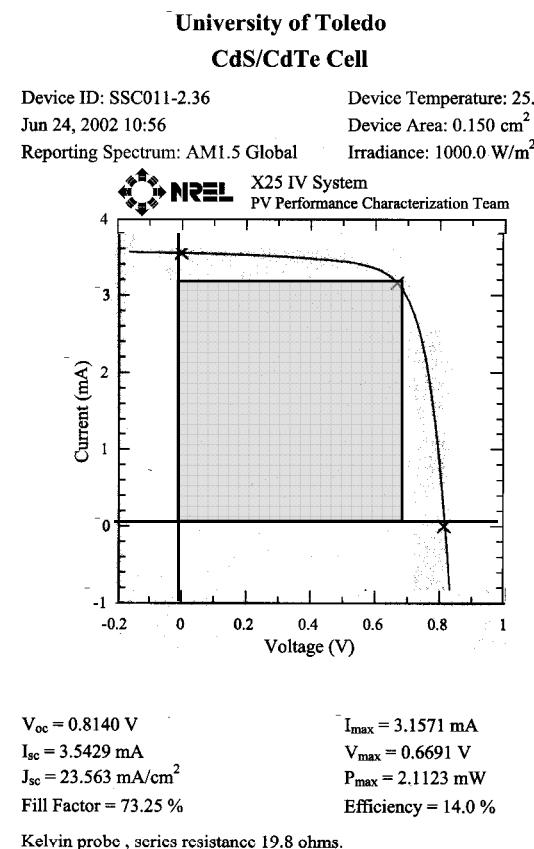
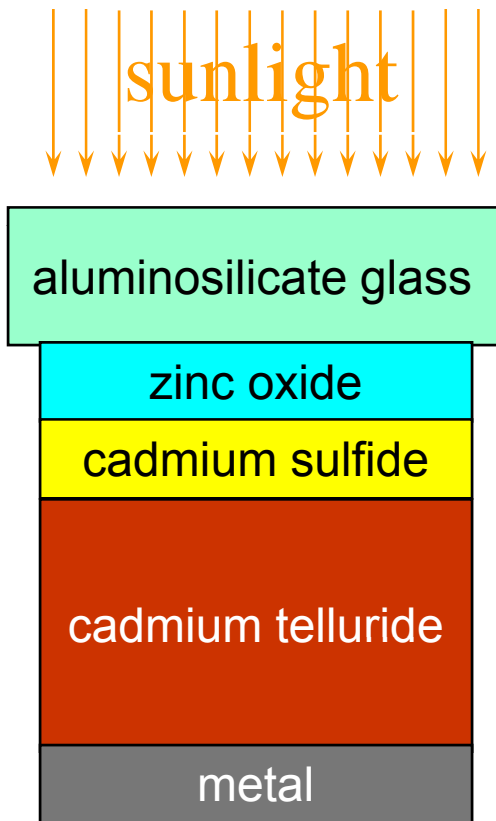
Band structure?

(Construct on board with class discussion)

- Cliff or spike at the CdS/CdTe interface?
- Doping densities?
- Back barrier?

UT CdTe sputtered cell on aluminosilicate glass

14.0% efficiency at one-sun illumination



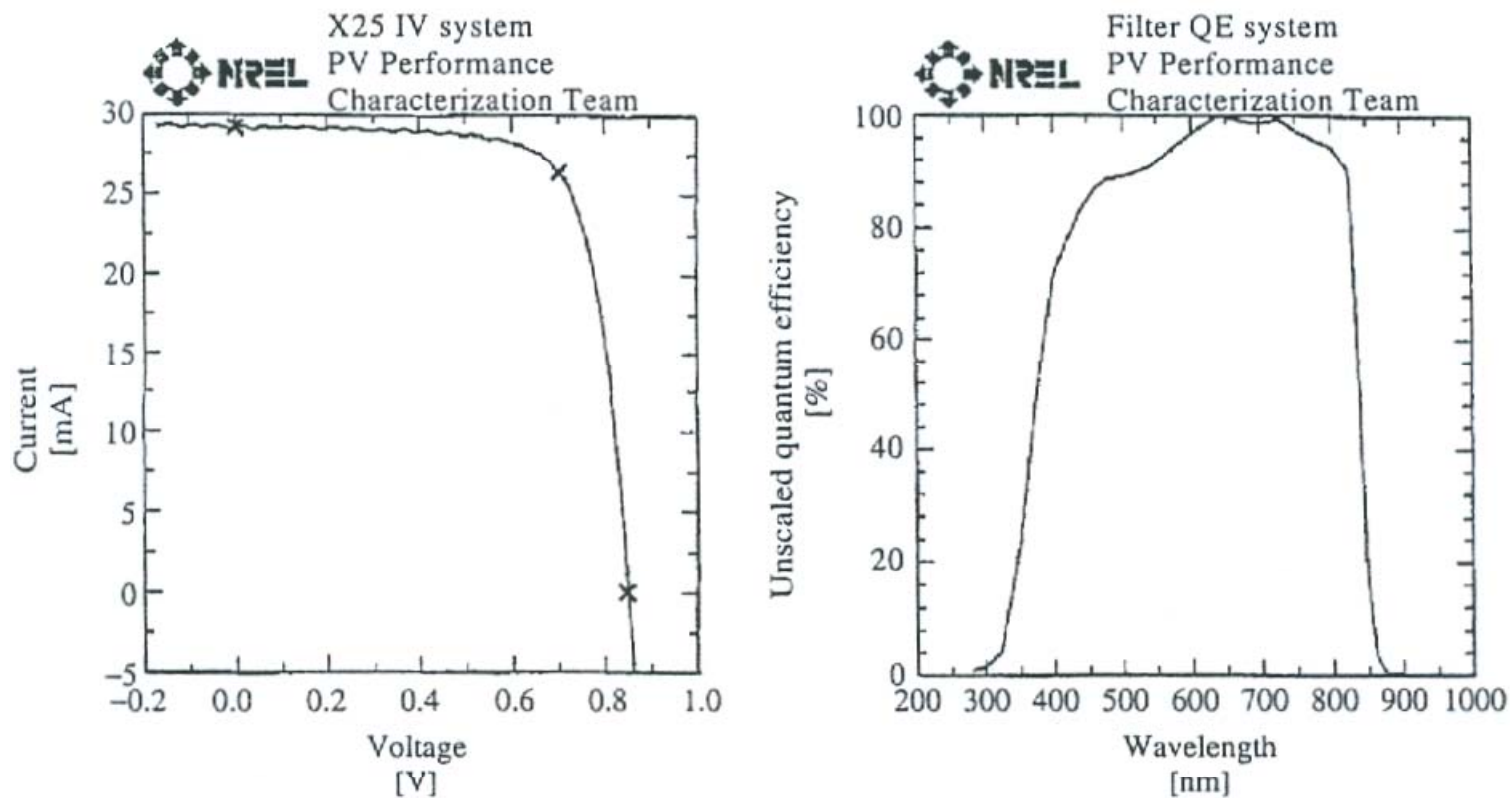
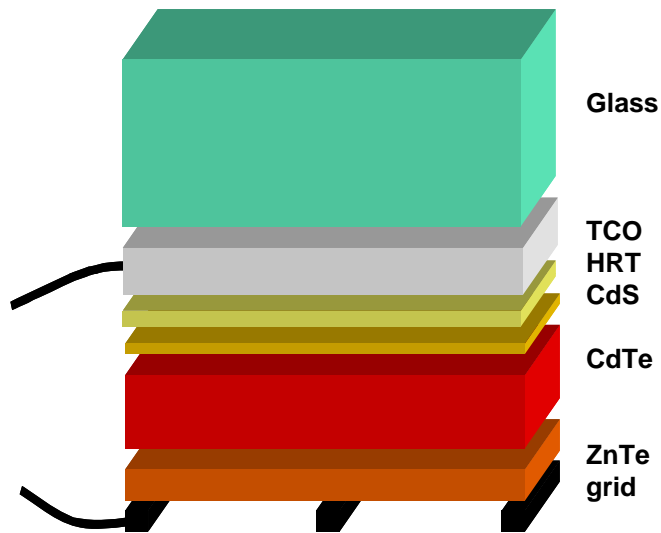


Figure 14.2 Current–voltage and relative quantum efficiency curves for 16.4%-efficient CdTe/CdS 1-film solar cell [37]

From B.E. McCandless and J.R. Sites, PV Handbook, 2002



Typically the back contact is a metal or carbon paste rather than the transparent ZnTe shown here.

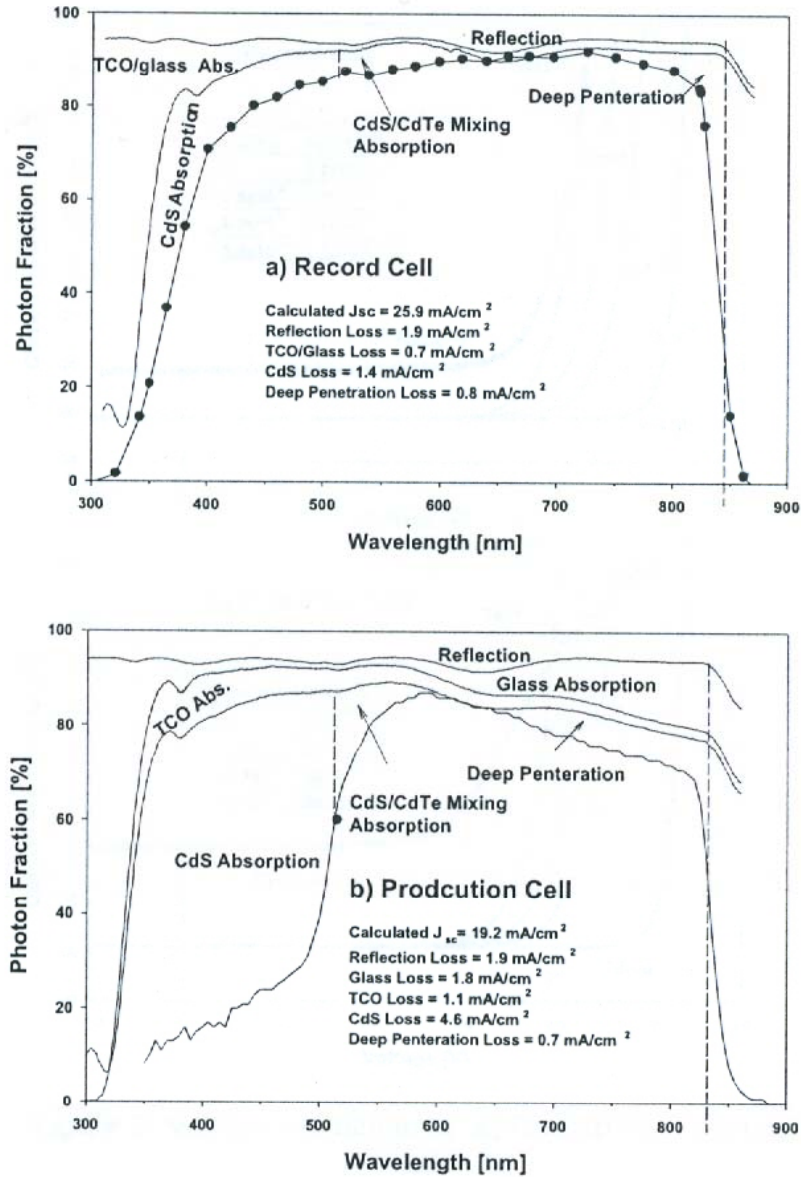


Figure 2. Photon accounting for a) Record cell
 b) Production cell.

Note on slide 11 particularly the following:

- Loss due to CdS absorption
- Loss due to intermixing
- Increased red response due to intermixing

PL in CdS/CdTe junctions (from D-H Kwon)

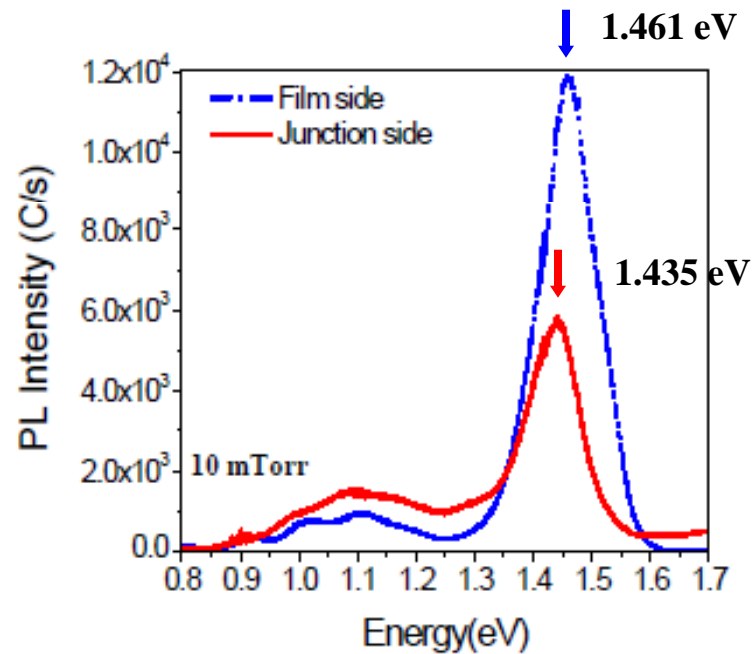


Fig10. Film and Junction side PLs of the same film

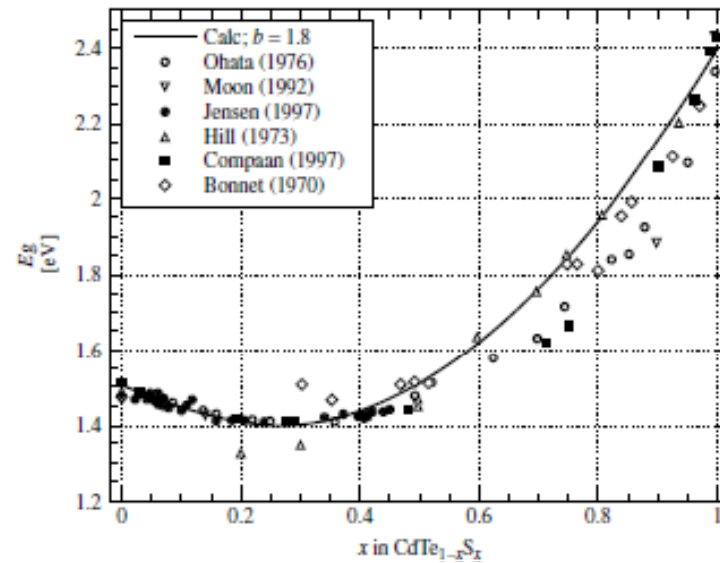


Fig 11. Optical bandgap of $\text{CdTe}_{1-x}\text{S}_x$ alloy thin films versus composition.

- Film side and junction side PL at 10 K from as-deposited cells
- Intermixing of S at the junction changes the bandgap of the material and ratio of S can be indirectly estimated

Fig. 10 from: DoHyung Kwon, X. Liu, N. R. Paudel, K. A. Wieland, and A. D. Compaan, “INFRARED PL STUDIES OF SPUTTERED CdTe FILMS AND CELLS”, 35th IEEE PVSC conference proceedings, June 2010

Fig. 11 from: Antonio Luque and Steven Hegedus, “Handbook of Photovoltaic Science and Engineering”, p638, Wiley, West Sussex England, 2003

From B.E. McCandless and J.R. Sites, PV Handbook, Chap 14, 2002

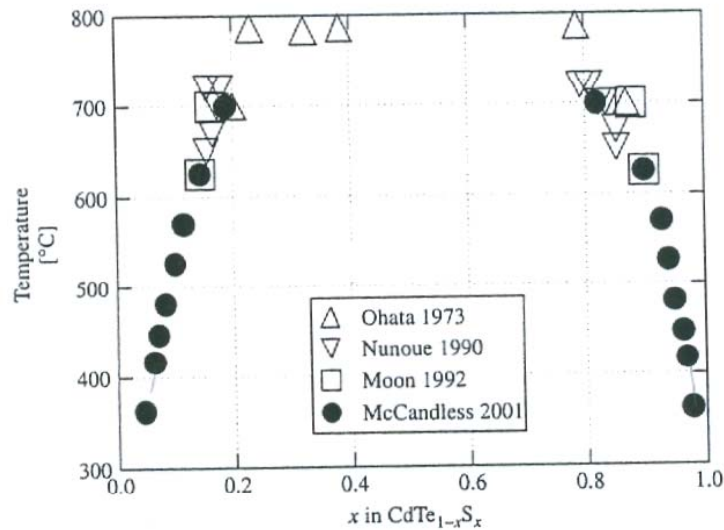


Figure 14.14 CdTe–CdS pseudobinary phase diagram. (Data listed in order from References [72, 139, 144, 147])

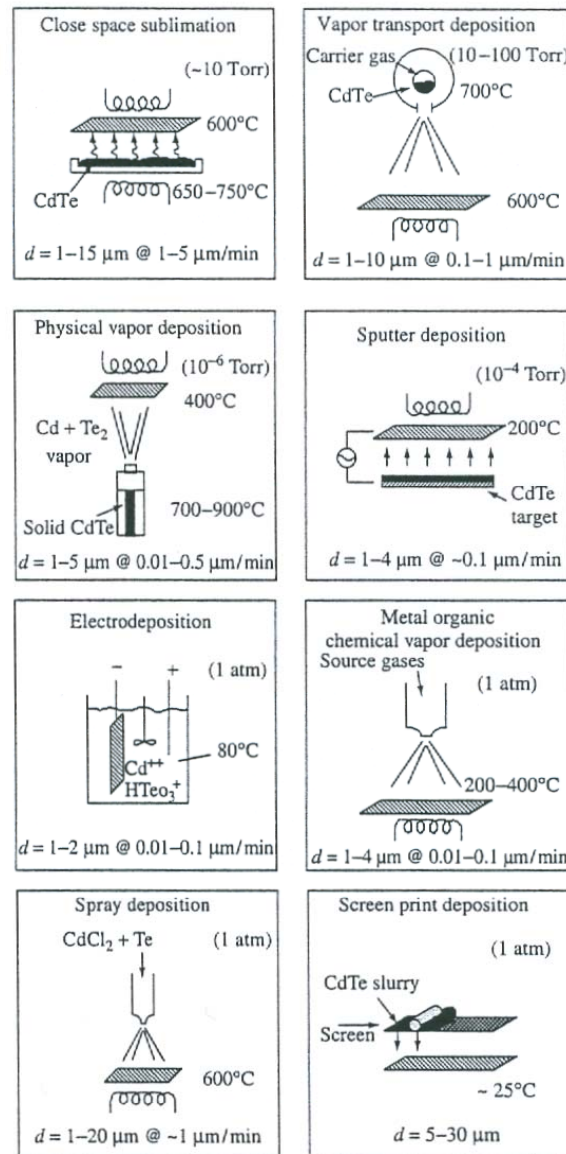


Figure 14.6 Schematic representations of eight CdTe thin-film deposition techniques. The substrate in each view is the cross-lined rectangle. Film thickness, d , and growth rate are shown at the bottom of each panel

Calculated impurity levels in CdTe

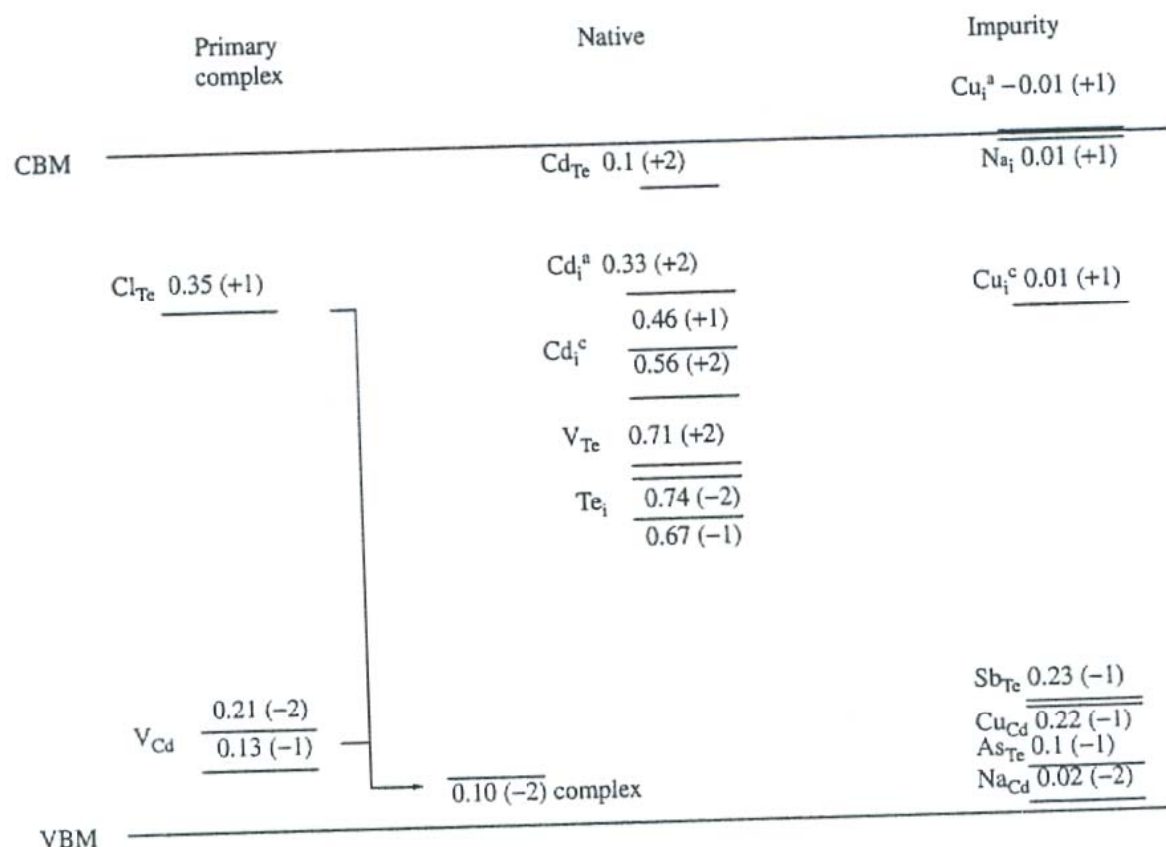
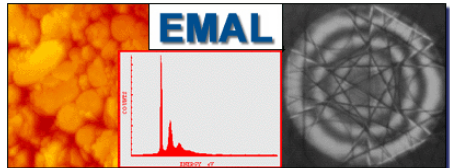


Figure 14.5 CdTe band structure with doping and defect levels. Charge states are in parentheses; energy is in electron volts measured from the conduction band for donor (positive) states and valence band for acceptor (negative) states. The superscripts a and c represent alternative interstitial sites. (Adapted from Wei S, Mtg. Record, National CdTe R&D Team Meeting (2001) Appendix 9 [59])

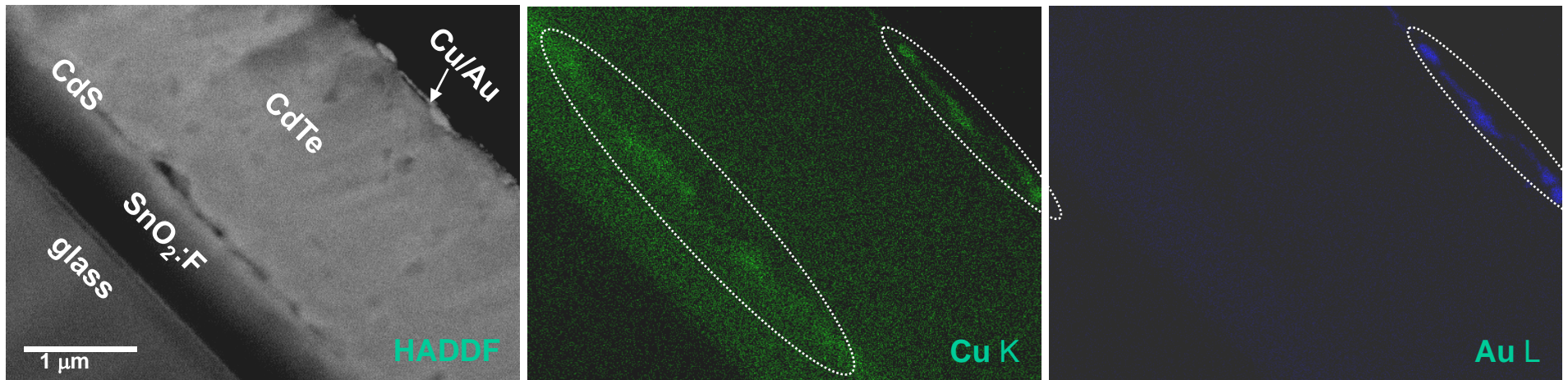
Discuss Cu distributions

- Secondary Ion Mass Spectroscopy
(usually done in conjunction with ion beam etching for depth profiling)
- Cu is used in the back contact
- CdCl₂ “activation” anneal is used just prior to the back contact deposition
- CdCl₂ activation is done in the presence of O₂ at 387 C



- small spot XRF data from Umich's EMAL

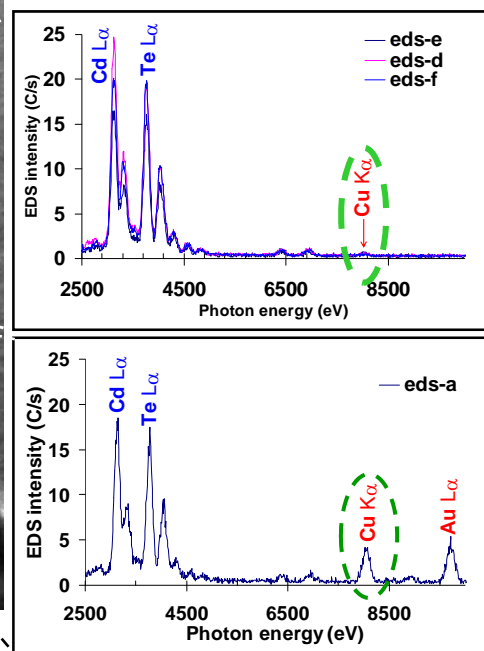
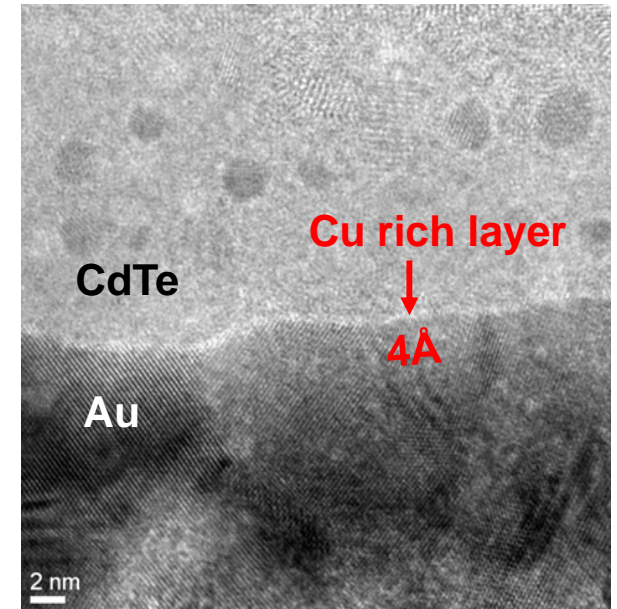
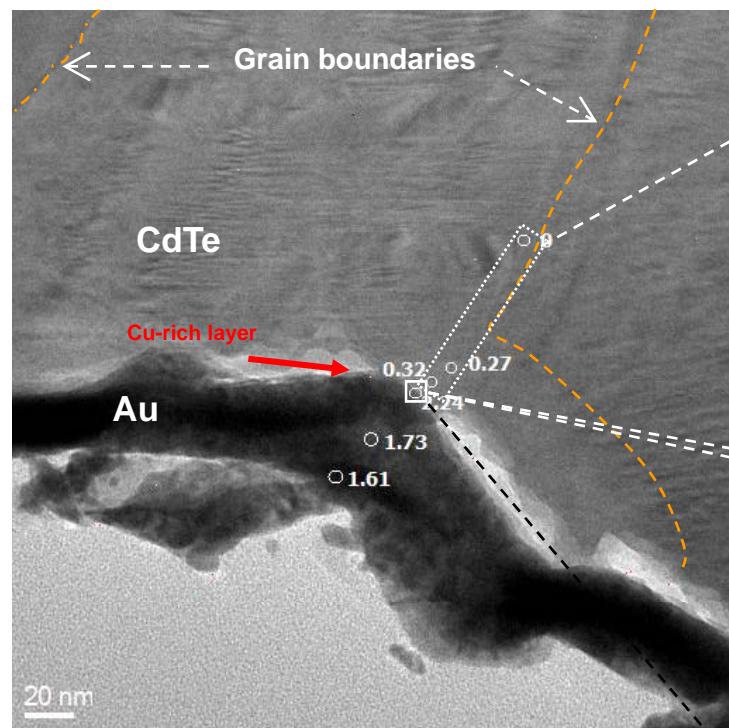
EDS mapping and High Angle Annular Dark Field (HAADF)



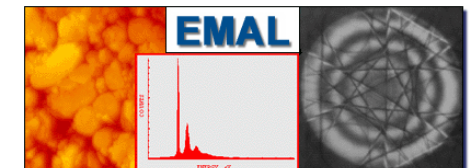
1. A high concentration of Cu at back contact
2. Au layer has high Cu content, Cu-Au alloy phases
3. Relatively high concentration in the CdS layer and some in $\text{SnO}_2:\text{F}$ accounts for most of the ~10% Cu diffused from the back contact.

Little evidence for Cu concentrated at grain boundaries: XTEM with small spot EDS

- evidence of some voids near the CdS/CdTe interface
- high Cu concentration at interface and in the Au layer
- little evidence of Cu along grain boundaries

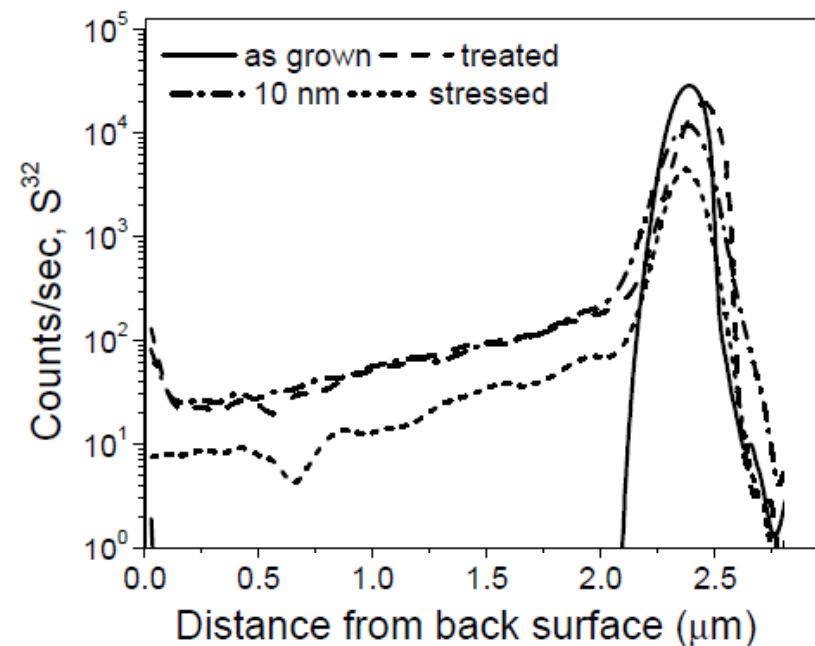
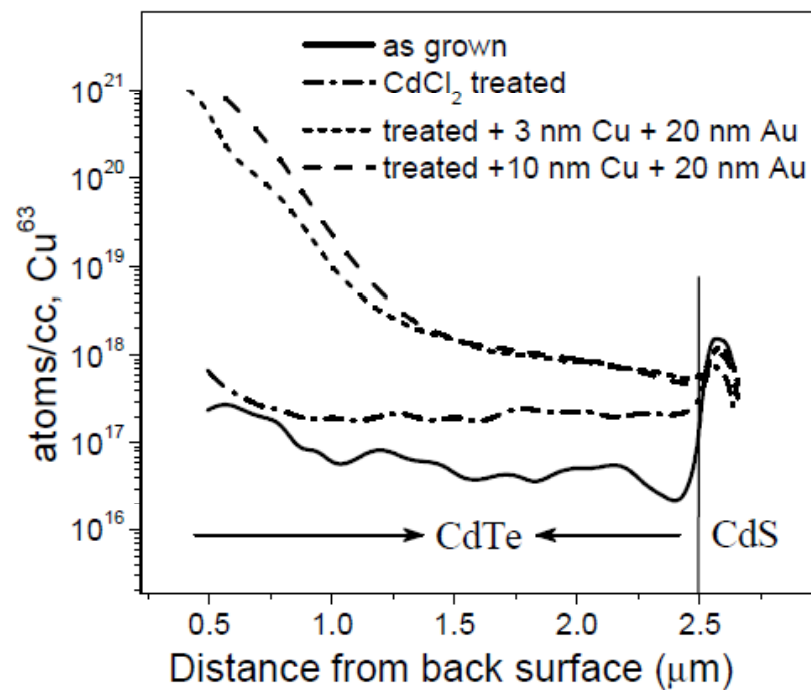


Data obtained in
collaboration with Kai Sun
UMich EMAL.

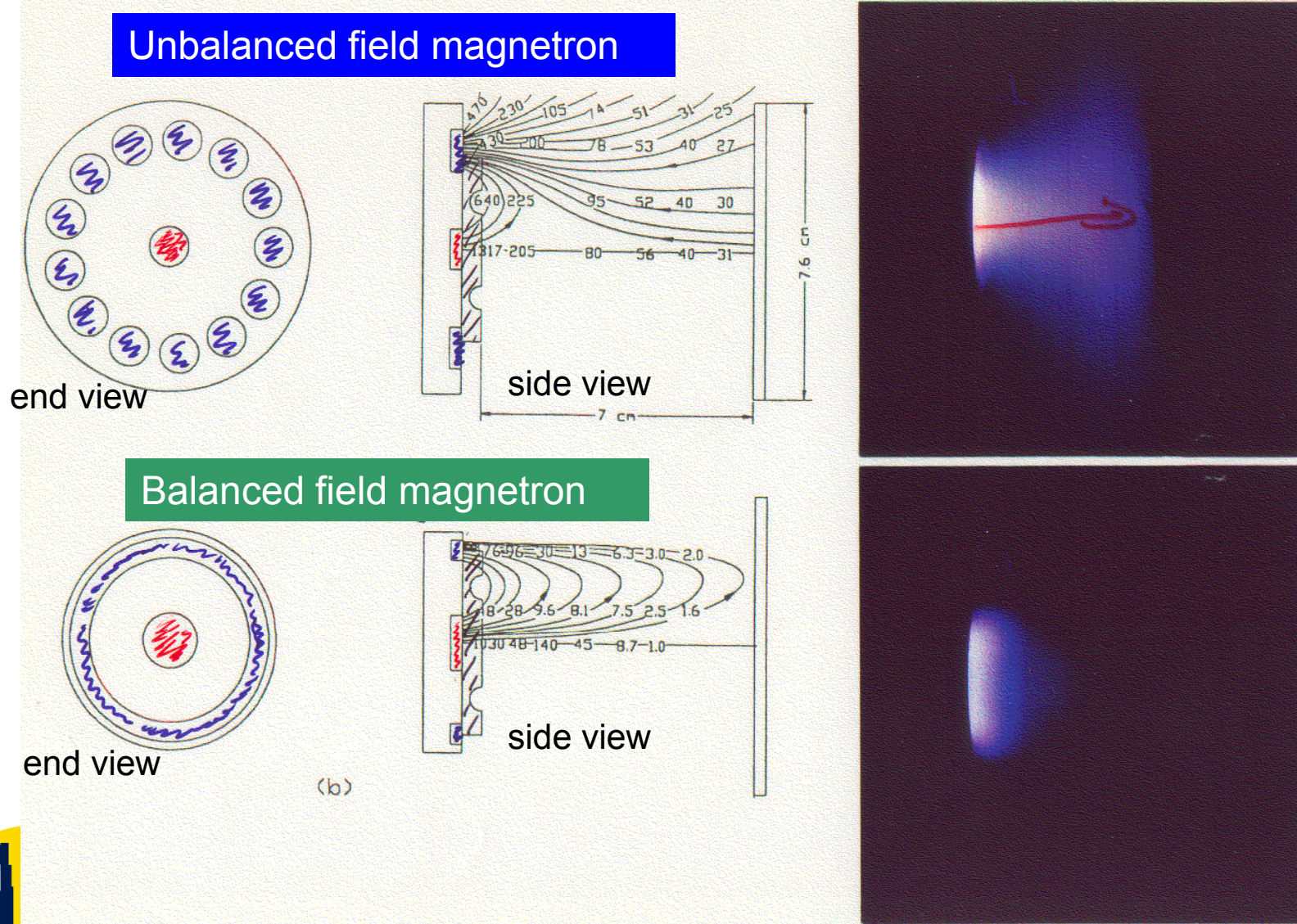


SIMS profiles of Cu and S in CdTe/CdS

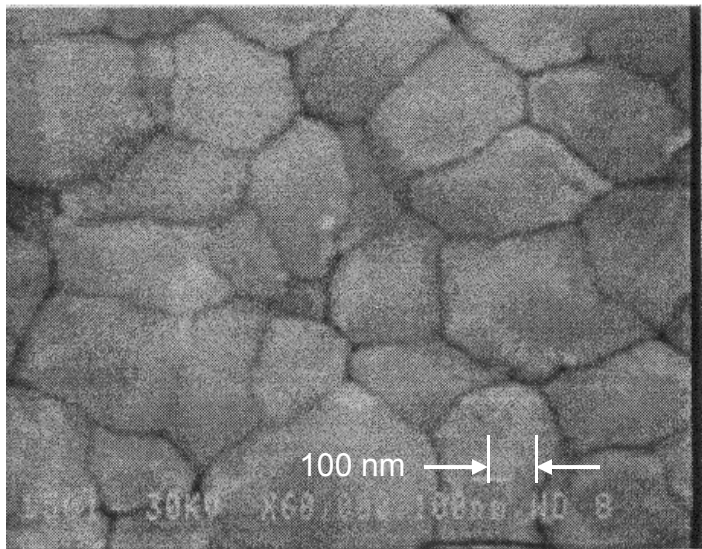
(data from Matt Young and Sally Asher (NREL))



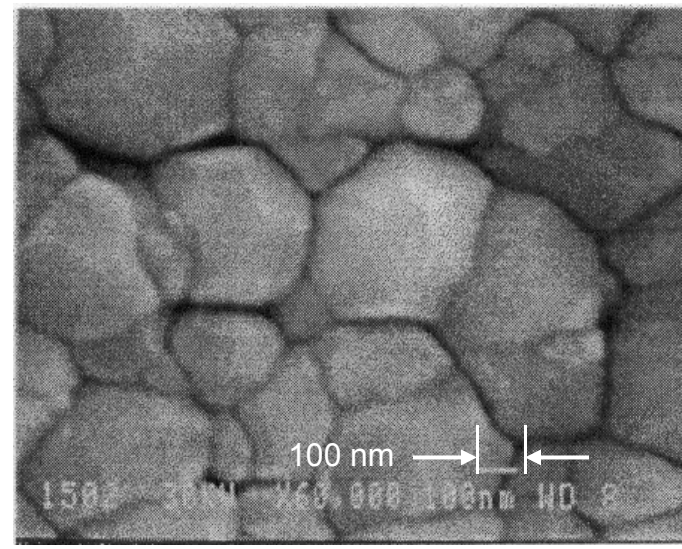
Plasma dependence on magnetic field



Grain morphology vs magnetron B-field



Strongly **unbalanced** gun (39,1),
CdTe: 25 W RF, 300 C, 18 mT



Nearly **balanced** gun (13,12),
CdTe: 25 W RF, 300 C, 18 mT

UT SEM data from magnetron-sputtered samples grown at UT

Grain boundaries: the challenge of polycrystalline thin- film cells

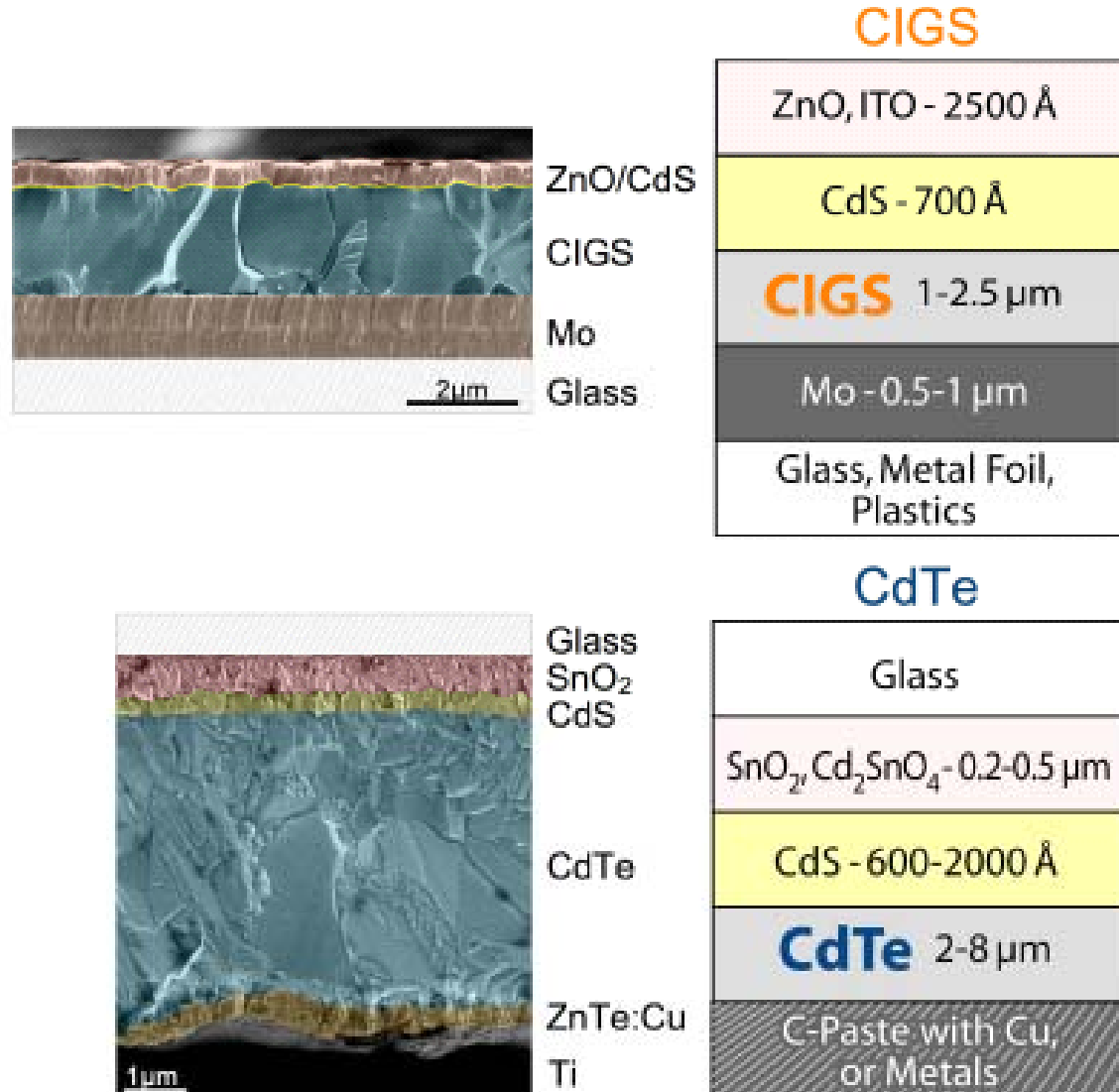


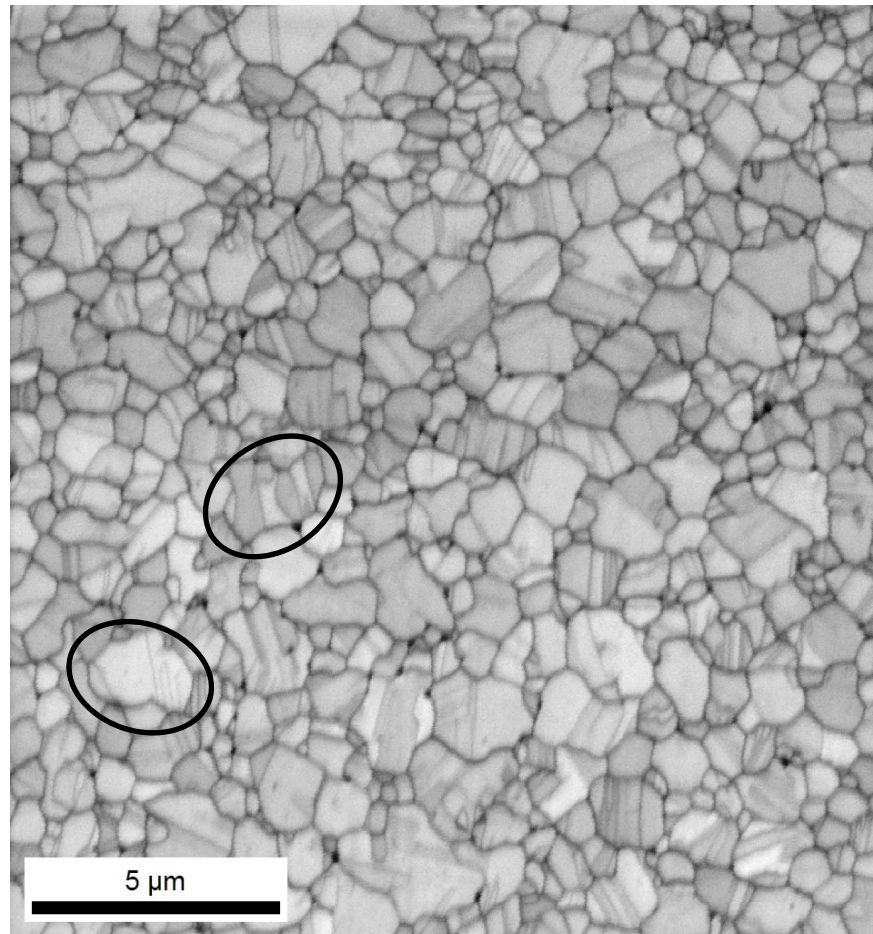
Fig. 4.2 Structure of the polycrystalline CIGS and CdTe cells.
From Noufi 2006.

EBSD data of grain size and low-angle grain boundaries

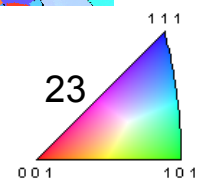
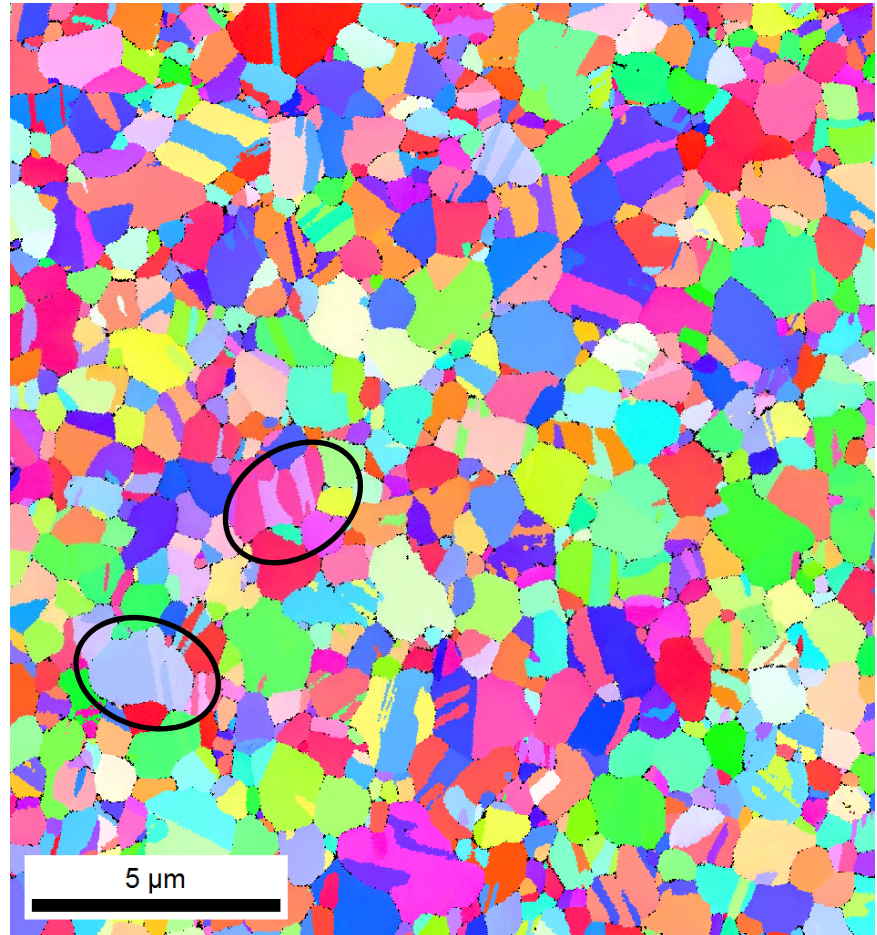
(Data taken on UT cell SSC548 by Matt Nowell of EDAX-TSL / U. Utah)

(sputtered CdTe-center region CdCl₂ treated)

secondary electron Image



EBSD orientation map

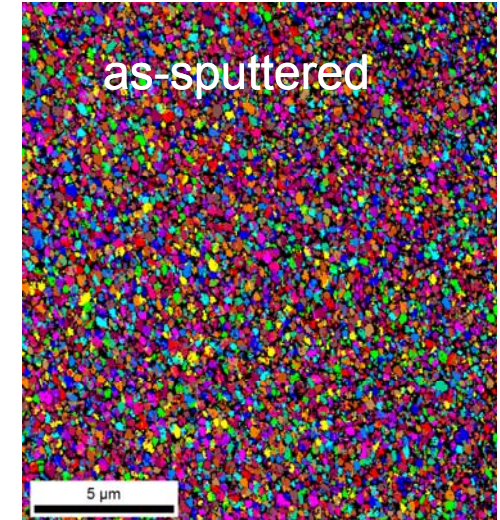
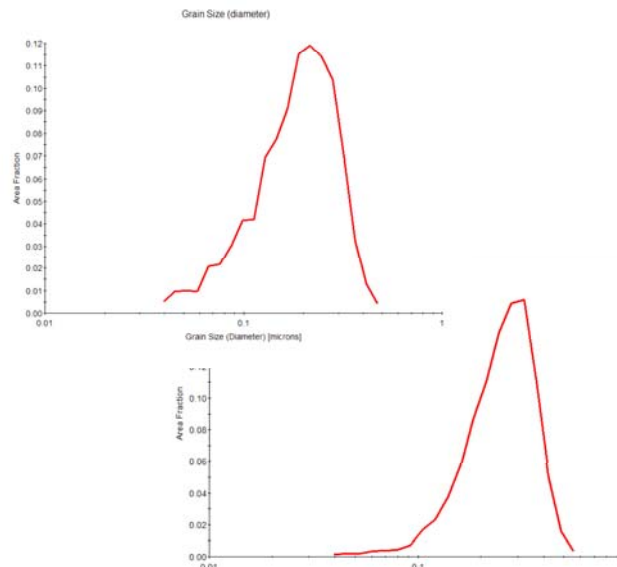


Grain size increases with CdCl_2 activation: EBSD

Data from Matt Nowell of EDAX-TSL / U. Utah obtained on UT films

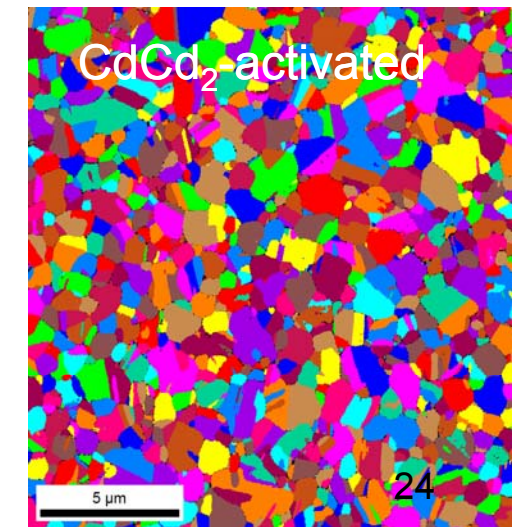
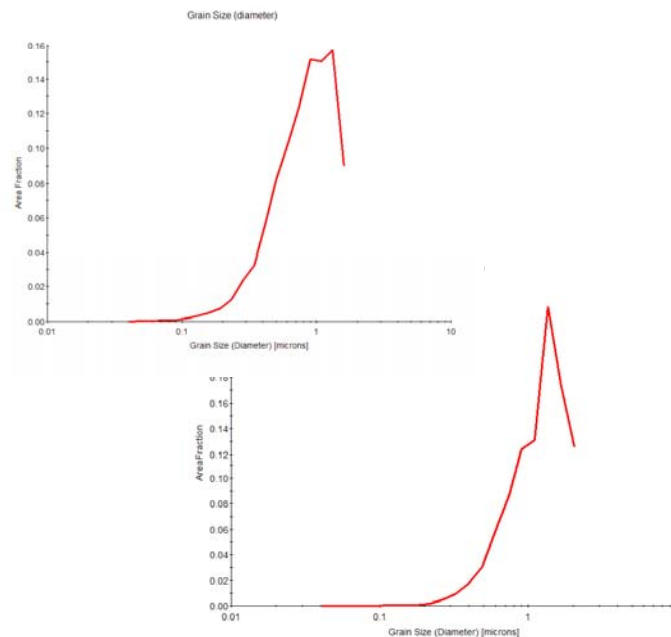
SSC548 Center As-Grown

- Grain map and size distribution **including** twins (ave. grain size = 115 nm)
- Grain map and size distribution **excluding** twins ($\Delta\theta < 5^\circ$) (ave. grain size = 176nm)



SSC548 Center CdCl_2 treated

- Grain map and size distribution **including** twins (ave. grain size = 400 nm)
- Grain map and size distribution **excluding** twins (ave. grain size = 710 nm)

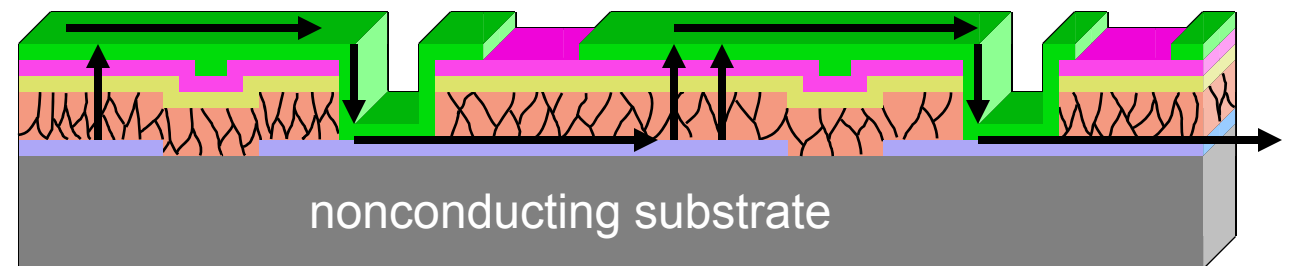




from cell to module--
series integration

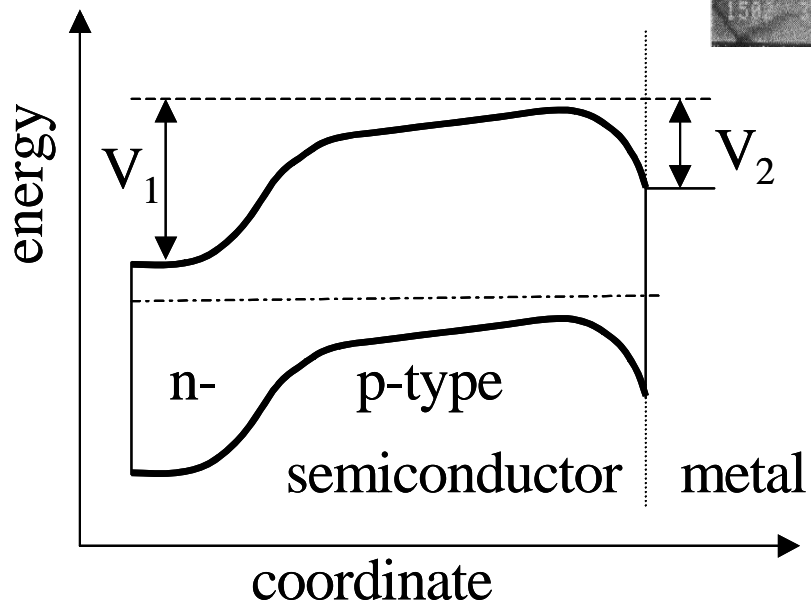
assembly from smaller cells

monolithic integration

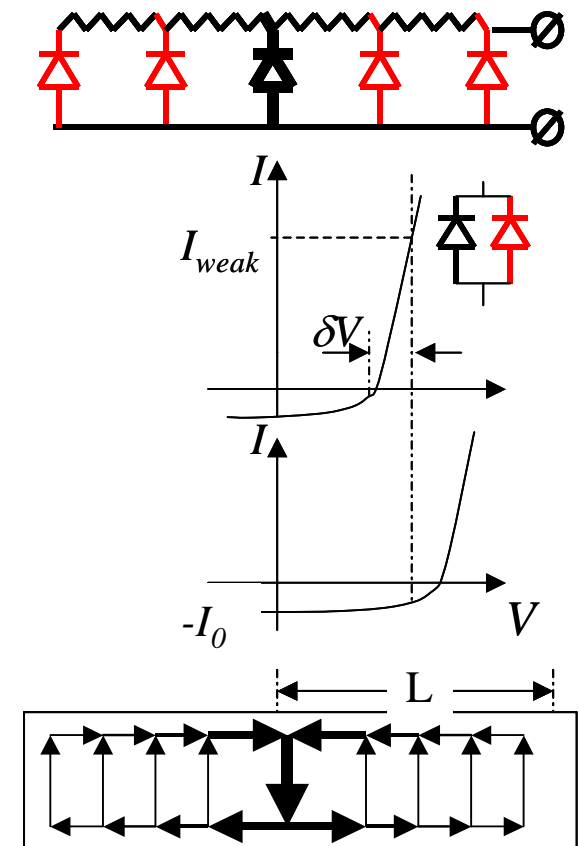
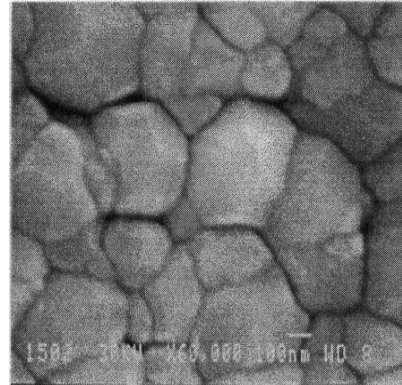


Diodes in parallel with variable performance

(model and analysis by Victor Karpov, Diana Shvydka of U. Toledo)



Schematic band diagram of the CdS/CdTe cell emphasizing the presence of a hole barrier, V_2 , at the back contact typically ~ 300 meV.



Elements of a random diode model which can result from variations in the back barrier leading to weak diodes which can shunt large amounts of current if the diodes are strongly linked with low resistance paths.